# A combined kinetico-mechanistic and computational study on the competitive formation of seven- versus five-membered platinacycles; the relevance of spectator halide ligands†

Gabriel Aullón,[a] Margarita Crespo,[*a] Mercè Font-Bardia,[b] Jesús Jover,[a] Manuel Martínez[*a] and Jack Pike[a]

aDepartament de Química Inorgànica, Universitat de Barcelona, Martí i Franquès 1-11, E-08028 Barcelona, Spain.
E-mail: margarita.crespo@qi.ub.es,
manel.martinez@qi.ub.es

bUnitat de Difracció de RX. Centres Científics i Tecnològics de la Universitat de Barcelona (CCiTUB). Universitat de Barcelona., Solé i Sabarís 1-3, 08028-Barcelona, Spain

The metalation reactions between [Pt2(4-MeC6H4)4(μ-SEt2)2] and 2-X,6-FC6H3CHvNCH2CH2NMe2 (X = Br, Cl) have been studied. In all cases, seven-membered platinacycles are formed in a process that involves an initial reductive elimination from cyclometallated PtIV intermediate compounds, [PtX(4-CH3C6H4)2(ArCHvNCH2CH2NMe2)] (X = Br, Cl), followed by isomerization of the resulting PtII complexes and a final cyclometallation step. For the process with X = Br, the final seven-membered platinacycle and two intermediates, isolated under the conditions implemented from parallel kinetic studies, have been characterized by XRD. Contrary to previous results for the parent non-fluorinated imine 2-BrC6H4CHvNCH2CH2NMe2 the presence of a fluoro substituent prevents the formation of the more stable five-membered platinacycle. Temperature and pressure dependent kinetico-mechanistic and DFT studies indicate that the final cyclometallation step is strongly influenced by the nature of the spectator halido ligand, the overall reaction being much faster for X = Cl. The same DFT study conducted on the previously studied systems with imine 2-BrC6H4CHvNCH2CH2NMe2 indicates that, when possible, fivemembered platinacycles are kinetically preferred for X = Br, while the presence of Cl as a spectator halido ligand leads to a preferential faster formation of seven-membered analogues.

## INTRODUCTION

Reductive elimination reactions have attracted a great deal of interest since they may lead to the formation of new bonds, in either stoichiometric or catalytic transformations. In particular, Pt(IV) compounds are considered adequate models to study reductive elimination processes from d6 octahedral complexes. Recent findings based on reductive elimination from platinum(IV) complexes include the formation of C–C and C–halide bonds1 and a catalytic process for conversion of a C–F bond into a C–C bond.2 In particular, cyclometallated platinum(IV) compounds [PtXR2(Ar′CHNCH2CH2NMe2)] or [PtXR2 (Ar′CHNCH2Ar′)L] containing respectively a tridentate [C,N,N′] ligand or a bidentate [C,N] and a neutral monodentate L ligand can be easily obtained from the reactions of platinum precursors containing "PtR2" moieties and potentially tridentate or bidentate imine ligands, Ar′CHNCH2CH2NMe2 or Ar′CHNCH2Ar′. In recent years, we have been involved in studies related to the formation of platinum(II) cyclometallated compounds generated from the mentioned platinum(IV) cyclometallated compounds with tridentate [C,N,N′] amino–imine ligands, or bidentate [C,N] imine ligands, and a neutral monodentate ligand L.3–12 The interest in these reactions arises from the fact that along the process new C–C bonds are formed via an initial reductive elimination to give a noncyclometallated platinum(II) compound that, in the second step, evolves towards a cycloplatinated compound. Although a common sequence operates, this process is highly versatile since both the nature of the formed C–C bond and the structure of the final cyclometallated platinum(II) compound can be tuned by a judicious choice of both the platinum precursor "PtR2" and the imine ligand, Ar′CHNCH2CH2NMe2 or Ar′CHNCH2Ar′, used in the formation of the cyclometallated platinum(IV) compound. For instance, the reaction of [Pt2Me4(μ-SMe2)2] with imine ligands Ar′CHNCH2Ar′ leads to a cyclometallated platinum(IV) compound from which Caryl–Calkyl bonds are formed and the subsequent metalation can lead to either five or six-membered metallacycles corresponding to C–H activation at the aryl group of the imine, or at the methyl ligand of the platinum precursor, respectively (Scheme 1).3,5

For diarylplatinum precursors, the corresponding platinum(IV) compounds lead to the formation of Caryl–Caryl bonds from which either seven-membered platinacycles containing the new biaryl fragment or five-membered analogues, in which the newly formed C–C bond is outside the metallacycle, can be obtained.4,6,7,9–12 For the former, C–H bond activation takes place at the aryl ligand of the precursor, while for the latter this process takes place at the aryl ring of the imine. A clear example (Scheme 2) is obtained when cis-[Pt(C6F5)2(SEt2)2] is used, since, in this case, the ortho-fluorine substituents preclude the formation of seven-membered platinacycles, due to the low reactivity of C–F bonds, and therefore the reaction is directed towards the formation of five-membered analogues.8

A more striking result, shown in Scheme 3, was obtained in the reaction of [Pt2(4-MeC6H4)4(μ-SEt2)2] with imines 2-XC6H4CHvNCH2CH2NMe2 (X = Br or Cl) since, in this case, the nature of the halide is determinant: a five-membered platinacycle is obtained for X = Br, while a seven-membered platinacycle is produced for X = Cl. This system has been thoroughly studied from a kinetico-mechanistic point of view and although formation of a seven-membered platinacycle for X = Br was found plausible under harsher conditions, the compound could not be obtained in a pure form.4

Since seven-membered platinacycles are a novel class of compounds with potential interest associated with their cytotoxic properties,13,14 in addition to the intrinsic interest based on the formation of biaryl linkages, we decided to explore novel strategies in order to analyse whether it would be possible to obtain such compounds even when X = Br. In this work, the reactions of [Pt2(4-MeC6H4)4(μ-SEt2)2] with imines 2-X,6-FC6H3CHvNCH2CH2NMe2 (X = Br or Cl) have been studied with the idea that the fluoro substituent at the ortho position in the aryl ring of the imine ligand should prevent the C–H bond activation at the imine and thus, in both cases, the reaction would be driven towards the formation of seven-membered platinacycles rather than five-membered analogues. It should be noted that five-

membered metallacycles are more stable than other ring products and generally cyclometallation reactions take place with high regioselectivity to produce fivemembered rings.15–17 Kinetico-mechanistic and DFT studies of these types of systems should allow studying the effect of the nature of the halide (Br versus Cl) in the formation of sevenmembered platinacycles.

## RESULTS AND DISCUSSION

### Preparation and characterisation of compounds

Initial platinum(IV) compounds [PtX(4-MeC6H4)2(2-FC6H3CHv NCH2CH2NMe2)] (5-IV-X,F, X = Br and Cl; Scheme 4) were prepared in high yields, following previously established procedures, from [Pt2(4-MeC6H4)4(μ-SEt2)2] and imines 2-X,6- FC6H3CHvNCH2CH2NMe2 (X = Br and Cl).18 For X = Br the reaction was faster and was complete within 24 hours in toluene solution at room temperature, while for X = Cl the reaction requires 48 hours under the same conditions. As expected from the lower reactivity of C–F bonds, activation of this bond was not observed in either reaction. Using shorter reaction times, isolation and characterisation of the coordination compound [Pt(4-MeC6H4)2(2-F,6-ClC6H3CHvNCH2CH2NMe2)], formed prior to the intramolecular C–Cl bond activation has also been achieved; isolation of the corresponding bromo analogue has not been possible. In this case the intramolecular C–Br bond activation occurred readily after coordination of the imine ligand to platinum. All the isolated compounds were characterized by 1H and 19F NMR spectra, which were consistent with the expected structures as well as from the data available for analogous compounds.4,9 As expected, the J(Himine–Pt) values observed for the platinum(IV) compounds (45.6 and 46.0 Hz) are lower than those observed for the platinum(II) compound [Pt(4-MeC6H4)2(2-F,6-ClC6H3CHvNCH2CH2NMe2)] (50.8 Hz). For the latter, the J(Himine–Pt) value is consistent with both an E conformation of the imine moiety and the presence of an aryl ligand trans to this group.4 A set of signals of very low intensity that could not be fully assigned indicated also the presence of a Z isomer in the sample in small amounts (<5%).

When a toluene solution of compound 5-IV-Br,F was refluxed for 24 hours, the targeted seven-membered platinacycle [PtBr{(4-MeC6H3)(2-FC6H3)CHNCH2CH2NMe2}] (7-II-Br,F) was obtained. This compound could also be obtained in a onepot process from [Pt2(4-MeC6H4)4(μ-SEt2)2] and the corresponding 2-Br,6-FC6H3CHvNCH2CH2NMe2 imine under the same conditions. These results indicate that the presence of an inert C–F bond in the imine ligand is an efficient strategy to drive the reaction towards the formation of seven-membered platinacycles. Formation of the analogue chlorido compound [PtCl{(4-MeC6H3)(2-FC6H3)CHNCH2CH2NMe2}] (7-II-Cl,F) took place much more readily, since refluxing in toluene for 6 hours either a solution of the platinum(IV) compound 5-IV-Cl,F or a mixture of [Pt2(4-MeC6H4)4(μ-SEt2)2] and imine 2-Cl,6-FC6H3CHvNCH2CH2NMe2, produced the desired compound. NMR data are in good agreement with those reported for analogous compounds with chlorido ligands.9,13 The high value obtained for 3J(Himine–Pt) (150.4 Hz) is consistent with both the E conformation of the imine and the presence of an halide trans to the imino group.4

Suitable crystals of compound 7-II-Br,F were grown from dichloromethane–methanol at room temperature, and XRD analysis was possible from the crystals obtained, showing that the structure is composed of discrete molecules separated by van der Waals distances (Fig. 1a); selected bond data are listed in Table 1. The complex shows a square-planar coordination of the platinum(II) with a terdentate [C,N,N′] unit and a bromo ligand. The metallacycle consists of a non-planar seven-membered system in which the biaryl fragment and the imine functionality are included. Bond lengths and angles are well within the range of values obtained for analogous compounds,9,13 the Pt–Br bond length being slightly longer than the reported Pt–Cl lengths for compounds of the same type. Most bond angles at platinum are close to the ideal value of 90°, and the smallest angle corresponds to the chelate N–Pt–N bite angle.

To confirm whether the formation of seven-membered platinacycles from the corresponding platinum(IV) cyclometallated compounds follows a common sequence, regardless of the presence of a chlorido or a bromido ligand, time-resolved experiments were conducted. A xylene solution of the complexes was monitored at different temperatures and times to ascertain the best set of conditions where the intermediates were present in representative amounts. Proton NMR studies revealed that after

stirring a solution of 5-IV-Br,F for 90 minutes at 70 °C, 90% of the sample had progressed to the dangling biphenyl intermediate form II-Br,F (Scheme 4). From the reaction mixture, suitable crystals of the intermediate could be obtained in its E form, allowing for full XRD characterization as its CH2Cl2 solvato species. The relatively low value of 3J(Himine–Pt) (35.6 Hz) is in the range expected for compounds with an aryl ligand trans to the imino group and an E conformation of the imine.4 The molecular structure is also shown in Fig. 1b and selected molecular dimensions are listed in Table 1. The square-planar coordination of the platinum(II) is achieved with a bidentate [N,N′] ligand, a bromido, trans to the dimethylamino moiety, and a para-tolyl ligand. The bond lengths and angles are well within the range of values obtained for analogous compounds.4 Again, most of the bond angles at platinum are close to the ideal value of 90°, and the smallest angle corresponds to the chelate N–Pt–N bite angle. The crystal structure of this compound confirms that a biphenyl fragment involving a former para-tolyl ligand and the aryl ring of the initial ligand is formed from 5-IV-Br,F in a reductive elimination process.

As already reported, the compounds generated on reductive elimination on platinum(IV) compounds of the type 5-IV-X,Y may adopt four distinct isomeric forms (see Scheme 5); the aryl ring being trans to the amine or the imine moieties and with an E or Z imine conformation.4 By monitoring changes in the 1H NMR spectra of II-Br,F, under the conditions suggested by the kinetic experiments detailed in the next section, compound II′-Br,F, as a mixture of E and Z isomers in a proportion E : Z = 2 : 1, was obtained. As previously reported,4 the values of J(Himine–Pt), which in this case are 152 Hz and 84 Hz for the E and Z isomers, respectively, indicate the presence of an halide ligand trans to the imine. From this mixture, XRD quality crystals were obtained and analysed; the molecular structure is shown in Fig. 1c and selected molecular dimensions are listed in Table 1. This compound differs from the previously described intermediate in that the bromido ligand is now trans to the imino fragment, and the latter displays a Z arrangement. A careful examination of this Z isomeric form of the species results in clear evidence that this form cannot produce the final seven membered platinacycles for orientation reasons. A similar treatment carried out on compound II-Cl,F produced rather complex 1H NMR spectra which consist of mixtures of up to four possible isomers of the species plus the initial and final reaction compounds (i.e. 5-IV-Cl,F and 7-II-Cl, F). From these complex mixtures, already anticipated from the data collected in the next section, it was not possible to isolate any of the relevant species.

## Kinetico-mechanistic studies on the formation of sevenmembered 7-II-Br,F and 7-II-Cl,F metallacycles

The rather complex nature of both the possible reaction intermediates and the nature of the final cyclometallated complexes formed in the reactions is generalised in Scheme 5. This general scheme is clear both from some previous results already published,4,19 and those indicated in the previous section. Given the fact that time-resolved monitoring of the processes has been found to be a perfect handle to gain a better insight into the reaction mechanism, the UV-Vis monitoring of the transformation of complexes 5-IV-X,F has been conducted from a kinetic perspective.

For complex 5-IV-Br,F the spectral changes observed on monitoring 5 × 10−4 M xylene solutions at varying temperatures indicate the operation of a two-step process in the 2–24 hour range at 90 and 60 °C respectively. By using the standard software indicated in the Experimental section, these changes could be easily fitted to a consecutive set of two single exponentials. From the time scale, as well as from parallel NMR monitoring, and the preparative procedures indicated before these processes correspond to the reductive elimination from 5-IV-Br,F to II-Br,F followed by isomerisation to II′-Br,F. The follow up final reaction to produce 7-II-Br,F could not be monitored due to the high temperature needed as well as for its time scale. Table 2 collects the relevant kinetic and activation data derived from the plots shown in Fig. 2a for the processes monitored, together with other relevant data for similar processes. The data indicate that the mechanism operating for the full process perfectly parallels that found for the reactivity of the similar 5-IV-Br,H, although in the present case the formation of the final five-membered

platinacycle is hindered by the presence of the fluoro substituent at the remaining ortho position of the initial imine ligand. Formation of the seven membered 7-II-Br,F species is much slower, and it only occurs due to the blockage of the position leading to the 5-II-Br,H complex. From the thermal and pressure activation parameters it is clear that the reductive elimination reaction, i.e. 5-IV-Br,F → II-Br,F, requires a rather large activation enthalpy with practically no changes in entropy, which indicates a transition state with a dominant breaking of the two Pt–C bonds, but keeping them organised by an incipient C–C bond making. This is the behaviour expected for this type of general reductive elimination reactions. As for the volume of activation (Fig. 2b), it is in line with a small compression, precisely due to the new C–C bond being formed. As for the II-Br, F ⇄ II′-Br,F isomerisation reaction monitored, the activation parameters agree perfectly well with those obtained for the already studied II-Br,H ⇄ II′-Br,H process. The values of the entropy and volume of activation are very negative, in line with a rather ordered and compressed transition state. Probably the highest point in the energy of the process corresponds to the formation of the new Pt–NMe2 bond from a triangular-planar previously dissociated intermediate arrangement. Consequently, the value of the activation enthalpy for the process has to be rather low, as observed, given the non-limiting dissociation of the Pt–N bond.

The parallel study carried out on the 5-IV-Cl,F → 7-II-Cl,F process proved to be much more complex to be monitored. As indicated in the previous section, 1H NMR monitoring of the process according to the time-resolved changes obtained by UV-Vis indicated that the presence of a mixture of the four isomeric forms plus the final species indicated in Scheme 5 is prevalent under all the reaction conditions. The slowest process of the three step sequence observed was associated with the II-Cl,F ⇄ II′-Cl,F reaction, as an increase of concentration of the II′-Cl,F form is observed at this time-scale by 1H NMR monitoring; kinetics could be monitored with low methodological errors by UV-Vis. Contrarily, the initial fast reductive elimination reaction proved to be the most complicated to determine kinetically due to the low solubility of 5-IV-Cl,F in xylene at temperatures lower than 50 °C and the readiness of the process (see Table 2). Given the fact that the outcome of the full process under the conditions studied is the final 7-II-Cl,F the remaining step observed was associated with the oxidative II′-Cl,F → 7-II,Cl,F reaction. The kinetic and thermal activation parameters determined for all these sets of reactions are also indicated in Table 2 along with the results for the other relevant systems. Clearly the data agree very well with those observed for the similar systems studied. It is thus clear that the relative ease of formation of the final 7-II-X,F sevenmembered platinacycles is dictated by the presence of a X = Br or X = Cl donor in the II′-X,F → 7-II,X,F reaction, while the II-X, Y ⇄ II′-X,Y isomerisation process does not distinguish between the different X and Y donors on the platinum centre.

## DFT calculations

In view of the data collected in Table 2, DFT calculations have been conducted at 139 °C (xylene boiling point) in order to establish which of the reaction steps indicated in Scheme 5 could be responsible for the prevalence of the species 7-II-Cl,H and 7-II-Cl,Cl, while only the 5-II-Br,H complex is observed,4 instead of the expected 7-II-Br,H. The results should be then extrapolated to the present situation, 7-II-Cl,F and 7-II-Br,F, where complexes of type 5-II-Br,F are not possible due to the blocking design effect of the ligand used. Initial DFT calculations indicate that all E forms of II-X,H and II′-X,H are lower in energy than their corresponding Z analogues (Table 3). Since the reaction leading to the final products proceeds via the E isomeric form of the II′-X,H intermediates (vide infra), Z isomers can be considered irrelevant to the reaction course. Furthermore, as indicated in the previous sections, the distal C–H bond is too far away from the platinum(II) centre to be relevant for the oxidative addition process. From the data in Table 3 it is clear that the energies of the II′-X,H intermediates are in all cases lower than those of the II-X,H species, indicating that an isomerization process should be expected, as observed experimentally. The isomerization transition state (TS_Isom), involving a three coordinated platinum species with a dangling NMe2 group (Fig. S1†), was also calculated and found to be around

140 kJ mol−1 above II-X,H (see Table 3). The geometry of the calculated TS_Isom involves a rather late C–Pt–Nimine angle (180° (II-X,H) → 130° (TS_Isom) → 90° (II′-X, H)), in good agreement with the kinetic activation data obtained experimentally.

Once the most stable II′-X,H intermediate is formed, two possible selective parallel pathways, leading to the characterised metallacycles, are possible. The first one (Scheme 6, top) involves the oxidative addition of the C–HA bond at the platinum followed by the reductive elimination of toluene producing the five-membered platinacycle (5-II-X,H). The equivalent seven-membered platinacycle (7-II-X,H) would be obtained in a similar fashion whenever the C–HB bond is activated at the metal (Scheme 6, bottom). Given the fact that five-membered platinacycles are more stable than their seven-membered counterparts (the calculated free energy difference being 31.8 (X = Br) and 33.4 (X = Cl) kJ mol−1, as expected from simple standard considerations)17,19,20 the obtention of the larger seven-membered platinacycle from the II′-Cl,H intermediate has to be due to kinetic preferences.

A close look at the energy barriers calculated for the formation of 5-II-Cl,H and 7-II-Cl,H reveals that the seven-mem- bered product is, indeed, the favoured one. While the barriers obtained for the formation of the 5-II-Cl,H five-membered platinacycle are 128.4 (oxidative addition, TS_CHA) and 155.6 (reductive elimination, TS_RE1) kJ mol−1, the formation of the seven-membered platinacycle compound, 7-II-Cl,H, produces 149.8 (TS_CHB) and 149.1 (TS_RE2) kJ mol−1 equivalent barriers, which imply the lower overall energy requirements. For the bromido analogues the outcome of DFT calculations produces the opposite trend, with the barriers favouring the formation of the five-membered product (see Scheme 6). In this case the energy requirements for oxidative addition (TS_CHA) and reductive elimination (TS_RE1) for the smaller five-membered platinacycles are 119.6 and 141.5 kJ mol−1 respectively, slightly lower than those found for the seven-membered product: 146.4 (TS_CHB) and 145.1 (TS_RE2) kJ mol−1. It may be argued that the final products could also be obtained from the II-X,H isomeric form, but higher barriers were obtained for these pathways both for X = Br and X = Cl. Other possible pathways such as those involving the C–H activation on the tetracoordinated square planar platinum centre of II′-X,H, or σ-CAM processes21 leading to the final products, were also computed and found to be noncompetitive with the mechanism proposed here.

The results collected in Scheme 6, which are clearly in line with the experimental observations, have been used to build a qualitative kinetic simulation model of product formation over time. For this purpose, the relative free energy differences have been transformed into rate constants by using the Eyring–Polanyi equation (i.e. $k = (kbT/h)\exp(-\Delta G‡/RT)$), and the product evolution over time, from II′-X,H, has been calculated (Fig. 3). As may be observed, at 139 °C the product distribution trend matches the experimental observations: 5-II-Br,H is produced with preference to 7-II-Br,H from II′-Br,H, whereas the inverse (7-II-Cl,H preferably to 5-II-Cl,H) is observed for II′-Cl, H. Although the time scale in Fig. 3 reasonably matches the values for X = Br (50% conversion after 24 h), for X = Cl there is more than an order of magnitude difference. Nevertheless, in this high energy range, this difference is easily overcome when the methodological errors involved in the DFT calculation (4–16 kJ mol−1) are taken into account.

The validity of the mechanism in Scheme 6 has also been confirmed by its use in the formation of the fluorinated compounds 7-II-Br,F and 7-II-Cl,F characterised in the present work, for which the formation of the five-membered platinacycle 5-II-X,F is not possible. The calculated energy requirements (Table S2†), although very similar, are slightly lower for the X = Cl system, indicating that the formation of 7-II-Cl,F should be definitively faster. In fact, the qualitative kinetic model indicates that 7-II-Cl,F is obtained around four times faster than 7-II-Br,F, practically the same difference as observed experimentally (Fig. S2†).

## CONCLUSIONS

In this work, the mechanism of formation of seven-membered platinacycles, in preference to the more thermodynamically stable five-membered analogues, has been disclosed through combined kinetico-mechanistic and computational studies. Seven-membered platinacycles are formed as the kinetically favoured products in a process which involves the reductive elimination from cyclometallated platinum(IV) compounds [PtX(4-CH3C6H4)2(ArCHvNCH2CH2NMe2)] (X = Br, Cl), followed by isomerization of the resulting platinum(II) compounds plus a final cyclometallation step. The results indicated that the nature of the spectator halido ligand X (X = Br or Cl) is determinant in the platinacycle size of reaction products. The presence of a bromido ligand slows down the formation of seven-membered platinacycles in such a way that the formation of the five-membered analogue becomes competitive unless the required metalation site is blocked with a fluoro substituent. Both kinetico-mechanistic and computational studies indicate that, contrary to previous suggestions, the isomerization step is not significantly affected by the nature of the halido ligand. On the contrary, all data are consistent with the fact that the final cyclometallation step is only dependent on the nature of the spectator halido ligand and this step is responsible for the nature of the final products. Therefore, five-membered platinacycles are preferred for Br, while the presence of a Cl leads to the formation of sevenmembered analogues.

## EXPERIMENTAL

### General procedures

Microanalyses were performed at the Centres Científics I Tecnològics (Universitat de Barcelona). Electrospray mass spectra were performed at the Servei d'Espectrometria de Masses (Universitat de Barcelona) using a LC/MSD-TOF spectrometer usingH2O–CH3CN 1 : 1 to introduce the sample. NMR spectra were performed at the Unitat de RMN d′Alt Camp de la Universitat de Barcelona using a Mercury-400 spectrometer (1H, 400 MHz; 19F, 376.5 MHz) and referenced to SiMe4 (1H) or CFCl3 (19F). The δ values are given in ppm and J values in Hz. Abbreviations used: s = singlet; d = doublet; t = triplet; q = quartet; m = multiplet.

### Preparation of complexes

The compounds [Pt2(4-MeC6H4)4(μ-SEt2)2]22 and 2-Cl,6-FC6H3CHvNCH2CH2NMe2 23 were prepared as reported elsewhere. Compound 7-II-Cl,F has been previously reported.13

**2-Br,6-FC6H3CHvNCH2CH2NMe2 (Chart 1).** To a solution of N,N-dimethylethylenediamine (0.22 g, 2.4 × 10−3 mol) in toluene was added 2-bromo,6-fluorobenzaldehyde (0.50 g, 2.7 × 10−3 mol), and the solution was allowed to stir at room temperature for 70 minutes. The mixture was dried over Na2SO4, the solution was filtered, and the solvent was removed under vacuum to give the product. Yield: 0.65 g (97%). 1H NMR (CDCl3, 298 K), δ: 8.47 [s, 1H, H1]; 7.40 [dd, 1H, 3J(H2–H4) = 8.0, H2]; 7.20 [td, 1H, 3J(H3–H4) = 3J(H3–F) = 8.0, 4J(H3–H2) = 5.6, H3]; 7.08 [td, 1H, 3J(H4–H2,3) = 8.0, H4]; 3.82 [t, 2H, 3J(H5–H6) = 6.8, H5]; 2.69 [t, 2H, 3J(H6–H5) = 7.0, H6]; 2.32 [s, 6H, H7]. 19F NMR (CDCl3, 298 K), δ: −111.70 [dd, 3J (F–H) = 10.4, 4J (F–H) = 6.0]. ESI-MS, m/z: 273.04 [M + H]+.

**[PtBr(4-MeC6H4)2{2-FC6H3CHvNCH2CH2NMe2}] (5-IV-Br,F, Chart 2).** A mixture of compounds [Pt2(4-MeC6H4)4(μ-SEt2)2] (100 mg, 1.06 × 10−4 mol) and 2-Br,6-FC6H3CHv NCH2CH2NMe2 (60 mg, 2.19 × 10−4 mol) was dissolved in 20 ml of toluene and was left for stirring at room temperature for 24 hours. The solvent was removed under vacuum to yield an oily residue. The oil was treated with diethyl ether and upon removal of ether under vacuum a yellow powder was obtained. Yield: 123 mg (89%). 1H NMR (CDCl3, 298 K), δ: 8.89 [s, 1H, 3J (Pt–H1) = 45.6, H1]; 7.55 [m, 2H, H2]; 6.94 [d, 2H, 3J(H3–H2) = 7.6, H3]; 6.70–6.65 [m, 4H, H4–H5]; 6.63 [m, 3H, H6–H8]; 4.46–4.37 [m, 1H, H9]; 4.36–4.23 [m, 2H, H10]; 2.97 [s, 3H, 3J (Pt–H11) = 11.2, H11]; 2.89–2.82 [m, 1H, H9′]; 2.50 [s, 3H, 3J (Pt–H11′) = 16.0, H11′]; 2.34 [s, 3H, H12]; 2.15 [s, 3H, H13]. 19F NMR (CDCl3, 298 K), δ: −112.38 [dd, 3J (F–H) = 10.9, 4J (F–H) = 5.6]. Anal. Found (calcd for C25H28BrFN2Pt): C: 45.9 (46.16); H: 4.7 (4.34); N: 4.4 (4.31).

**[PtBr{(4-MeC6H3)(2-FC6H3)CHvNCH2CH2NMe2}] (7-II-Br,F, Chart 3).** A solution of [Pt2(4-MeC6H4)4(μ-SEt2)2] (51 mg, 5.45 × 10−5 mol) and 2-Br,6-FC6H3CHvNCH2CH2NMe2 (30 mg, 1.10 × 10−4 mol) in 40 ml of toluene was stirred under reflux for 24 hours. The solvent was removed under vacuum to yield a yellow powder solid. Yield: 40 mg (65%). 1H NMR (CDCl3, 298 K), δ: 9.06 [s, 1H, 3J (Pt–H1) = 150.4, H1]; 7.55 [td, 1H, 3J(H2–H3,5) = 8.0, 4J(H2–F) = 6.0, H2]; 7.48 [d, 1H, 3J(H5–H2) = 8.0, H5]; 7.23 [s, 1H, H3]; 7.02 [ddd, 1H, 3J(H4–F) = 10.0, 3J(H4–H2) = 8.0, 4J(H4–H2) = 1.0, H4]; 6.85 [d, 1H, 3J(H6–H7) = 8.0, H6]; 6.78 [dd, 1H, 3J(H7–H6) = 8.0, 4J(H7–H4) = 1.6, H7]; 4.51 [m, 1H, 2J(H8–H8′) = 11.6, 3J(H8–H10,10′) = 4.4, 4J(H8–H1) = 1.2, H8]; 3.88 [m, 1H, 2J(H8′–H8) = 12.0, 3J(H8′–H10,10′) = 4.0, 3J (Pt–H8′) = 61.2, H8′]; 3.04 [s, 3H, H9]; 2.76 [s, 3H, H9′]; 2.70–2.56 [m, 2H, H10,10′]; 2.30 [s, 3H, H11]. 19F NMR (CDCl3, 298 K), δ: −118.62 [ddd, 3J (F–H) = 11.2, 4J (F–H) = 6.4, 5J (F–H) = 2.4]. Anal. Found (calcd for C18H20BrFN2Pt·H2O): C: 37.3 (37.51); H: 3.8 (3.85); N: 4.8 (4.86).

**[Pt(4-MeC6H4)2{(2-F,6-ClC6H3)CHvNCH2CH2NMe2}], (Chart 4).** A solution of [Pt2(4-MeC6H4)4(μ-SEt2)2] (199 mg, 2.13 × 10−4 mol) and 2-Cl,6-FC6H3CHvNCH2CH2NMe2 (98 mg, 4.28 × 10−4 mol) in 40 ml of toluene was stirred at room temperature for 4 hours. The solvent was removed under vacuum to yield yellow oil. The oil was treated with diethyl ether and upon removal of ether under vacuum a yellow powder was obtained. The yellow solid was recrystallised in dichloromethane–methanol to yield yellow crystals. Yield: 234 mg (91%). 1H NMR (CDCl3, 298 K), E-isomer, δ: 8.71 [s, 1H, 3J (Pt–H1) = 50.8, H1]; 7.24 [d, 2H, 3J(H2–H6) = 8.0, H2]; 6.97 [dt, 1H, 3J(H3–H4,7) = 8.0, 4J (F–H3) = 6.0, H3]; 6.80 [d, 1H, 3J(H4–H3) = 8.0, H4]; 6.73 [d, 2H, 3J(H5–H8) = 8.0, H5]; 6.69 [d, 2H, 3J(H6–H2) = 8.0, H6]; 6.54 [t, 1H, 3J(H7–H3) = 3J(H7–F) = 8.8, H7]; 6.17 [d, 2H, 3J(H8–H5) = 8.0, H8]; 4.15 [m, 2H, H9]; 2.78 [t, 2H, 3J(H10–H9) = 5.6, H10]; 2.63 [s, 6H, H11]; 2.13 [s, 3H, H12]; 1.90 [s, 3H, H13]. Z-isomer, 8.41 [s, 1H, 3J (Pt–H1) = 32.0, H1]; 2.64 [s, 6H, H11]; 2.18 [s, 3H, H12]. 19F NMR (CDCl3, 298 K), δ: −108.08 [dd, 3J (F–H) = 9.2, 4J (F–H) = 6.0]. Anal. Found (calcd for C25H28ClFN2Pt): C: 49.3 (49.55); H: 5.0 (4.66); N: 4.6 (4.62).

**[PtCl(4-MeC6H4)2{3-FC6H3CHvNCH2CH2NMe2}] (5-IV-Cl,F, Chart 5).** A solution of [Pt2(4-MeC6H4)4(μ-SEt2)2] (200 mg, 2.14 × 10−4 mol) and 2-Cl,6-FC6H3CHvNCH2CH2NMe2 (99 mg, 4.32 × 10−4 mol) in 40 ml of toluene was stirred at room temperature for 48 hours. The solvent was removed under vacuum to yield yellow oil. The oil was treated with diethyl ether and upon removal of ether under vacuum a yellow green powder was obtained. Yield: 208 mg (80%). 1H NMR (CDCl3, 298 K), δ: 8.90 [d, 1H, 4J(H1–H10) = 1.6, 3J (Pt–H1) = 46.0, H1]; 7.48 [d, 2H, 3J(H2–H6) = 8.0, H2]; 7.31 [m, 1H, H3]; 7.24 [dd, 1H, 3J(H4–H5) = 8.0, 4J(H4–H3) = 1.6, H4]; 7.09 [t, 1H, 3J(H5–H3,4) = 7.6, H5]; 6.95 [d, 2H, 3J(H6–H2) = 8.4, H6]; 6.73 [d, 2H, 3J(H7–H8) = 8.4, H7]; 6.64 [d, 2H, 3J(H8–H7) = 8.4, H8]; 4.45–4.35 [m, 1H, H9]; 4.34–4.20 [m, 2H, H10]; 2.85 [s, 3H, 3J (Pt–H11) = 11.2, H11]; 2.81–2.73 [m, 1H, H9′]; 2.51 [s, 3H 3J (Pt–H11′) = 16.0, H11′]; 2.34 [s, 3H, H12]; 2.15 [s, 3H, H13]. 19F NMR (CDCl3, 298 K), δ: −112.42 [dd, 3J (F–H) = 10.4, 4J (F–H) = 5.6]. Anal. Found (calcd for C25H28ClFN2Pt): C: 49.4 (49.55); H: 5.1 (4.66); N: 4.7 (4.62).

**E-[PtBr(4-MeC6H4){(4-MeC6H4)(2-FC6H3)CHNCH2CH2NMe2}] (II-Br,F, Chart 6).** Compound [PtBr(4-MeC6H4)2{3F-C6H3CHv NCH2CH2N(Me)2}] (5-IV-Br,F) (50 mg, 7.69 × 10−5 mol) was dissolved in 10 ml of toluene and stirred at 70 °C for 90 minutes. The solvent was removed to yield quantitatively a yellow solid (50 mg). The 1H NMR spectrum recorded in CDCl3 indicated 90% conversion of 5-IV-Br,F into II-Br,F. Recrystallization of the crude solid affords XRD quality crystals; a reproducible yield could not be obtained under these conditions. 1H NMR (CDCl3, 298 K), δ: 8.76 [s, 1H, 3J (Pt–H1) = 35.6, H1]; 7.49 [d, 2H, 3J(H2–H4) = 8.0, H2]; 7.44 [td, 1H, 3J(H3–H5,7) = 8.0, 4J (F–H3) = 5.6, H3]; 7.30 [d, 2H, 3J(H4–H2) = 8.0, H4]; 7.14 [dd, 1H, 3J(H5–H3) = 8.0, 5J(H5–H6) = 0.8, H5]; 7.10 [d, 2H, 3J(H6–H8) = 8.0, H6]; 7.09 [m, 1H, H7]; 6.77 [d, 2H, 3J(H8–H6) = 8.0, H8]; 3.84 [t, 2H, 3J(H9–H11) = 5.6, H9]; 2.73 [s, 3H, H10]; 2.61–2.54 [m, 2H, H11]; 2.47 [s, 3H, H10′]; 2.41 [s, 3H, H12]; 2.23 [s, 3H, H13].

**E/Z-[PtBr(4-MeC6H4){(4-MeC6H4)(2-FC6H3)CHNCH2CH2NMe2}] (II′-Br,F).** A solution of 10 mg of II-Br,F in toluene was heated at 90 °C for 24 hours. The solvent was removed and the 1H NMR spectrum was recorded in CDCl3, indicating a nearly quantitative conversion of II-Br,F into II′-Br,F. Recrystallization of the crude solid (9 mg) affords XRD quality crystals of the Z-isomer; a reproducible yield could not be obtained under these conditions. 1H NMR (CDCl3, 298 K), E-isomer, δ: 8.84 [s, 1H, 3J (Pt–H) = 152.0, H1]; 6.97 [d, 2H, 3J(H–H) = 8.0]; 6.62 [d, 1H, 3J(H–H) = 8.0]; 6.25 [d, 1H, 3J(H–H) = 8.0]; 4.23 [m, 2H]; 2.74 [s, 6H]; 2.41 [s, 3H]; 2.11 [s, 3H]. Z-isomer, δ: 8.22 [s, 1H, 3J (Pt–H1) = 84.0, H]; 7.43 [m, 1H]; 6.81 [d, 1H, 3J(H–H) = 8.0]; 6.58 [d, 1H, 3J(H–H) = 8.0]; 6.42 [d, 1H, 3J(H–H) = 8.0]; 3.42 [m, 2H]; 2.72 [s, 6H]; 2.44 [s, 3H]; 2.12 [s, 3H].

## X-ray structure analysis

Prismatic crystals were selected and intensity data were measured on a D8 Venture system equipped with a multilayer monochromator and a Mo microfocus. The structure was solved using the Bruker SHELXTL software package, and refined using SHELXL.24 All hydrogen atom positional parameters were computed and refined using a riding model, with an isotropic temperature factor equal to 1.2 times the equivalent temperature factor of the atom to which they are linked; further details are given in Table 4.

## Kinetics

The kinetic profiles for the reactions were followed by UV-Vis spectroscopy in the full 700–300 nm range on HP8452A or Cary50 instruments equipped with thermostated multicell transports. The observed rate constants were derived from absorbance versus time traces at the wavelengths where a maximum increase and/or decrease of absorbance were/was observed; alternatively the full spectral time—resolved changes where used. For the reactions carried out at varying pressures, the previously described pillbox cell and pressurising system25–28 were used and the final treatment of data was the same as described before. The calculation of the observed rate constants from the absorbance versus time monitoring of reactions, studied under first order concentration conditions, was carried out using the SPECFIT or RecatLab software.29,30 The general kinetic technique is that previously described.11,18,31 Table S1† collects the kobs values for all the systems studied as a function of starting complex, pressures and temperatures studied. All post-run fittings were carried out by using the standard available commercial programs.

## Computational details

All the structures have been optimized without restrictions in xylene using the B3LYP density functional32–34 including the D3 version of Grimme's dispersion35 as implemented in the Gaussian09 package.36 The standard 6-31G* basis set37–39 was used for all H, C, N, F, Cl and Br atoms; the Los Alamos National Laboratory double zeta basis set (LANL2DZ)39–41 along with the associated ECP describing the core electrons, was employed for Pt. The (IEF-PCM) method,42,43 including the radii and non-electrostatic terms for Truhlar and coworkers' SMD solvation model,44 was employed. In all cases, frequency calculations were carried out to confirm the nature of stationary points and transition states, with none and one negative value, respectively. Additional single point calculations on the optimized geometries were employed to obtain improved solvated free energy values with larger basis sets at 139 °C, the boiling point of xylene. The aug-cc-pVTZ basis set including polarization and the associated electron core potential45,46 was employed for Pt and Br whereas all the other atoms were described with the 6-311+G** all-electron basis set.45,47,48 All the free energy values reported in the text correspond to those obtained with the larger basis sets and can be found, along their relevant thermochemical terms, in Table S3.†

The kinetic models have been constructed with the Copasi software49 using the deterministic (LSODA) method with relative and absolute tolerance values of 10−6 and 10−12, respectively.

444 **ACKNOWLEDGEMENTS**

445

446 Financial support from the Spanish Ministerio de Economía y Competitividad (projects CTQ2012-
447 37821-C02-01 and CTQ2009-11501) is acknowledged.

448

## REFERENCES


1 A. Vigalok, Acc. Chem. Res., 2015, 48, 238–247. 2 T. Wang, L. Keyes, B. O. Patrick and J. A. Love, Organometallics, 2012, 31, 1397–1407.

3 C. M. Anderson, M. Crespo, N. Kfoury, M. A. Weinstein and J. M. Tanski, Organometallics, 2013, 32, 4199–4207.

4 P. V. Bernhardt, T. Calvet, M. Crespo, M. Font-Bardía, S. Jansat and M. Martínez, Inorg. Chem., 2013, 52, 474–484.

5 M. Crespo, C. M. Anderson, N. Kfoury, M. Font-Bardia and T. Calvet, Organometallics, 2012, 31, 4401–4404.

6 M. Crespo, M. Font-Bardia and T. Calvet, Dalton Trans., 2011, 40, 9431–9438.

7 M. Crespo, T. Calvet and M. Font-Bardia, Dalton Trans., 2010, 39, 6936–6938.

8 T. Calvet, M. Crespo, M. Font-Bardía, K. Gómez, G. González and M. Martínez, Organometallics, 2009, 28, 5096–5106.

9 R. Martín, M. Crespo, M. Font-Bardia and T. Calvet, Organometallics, 2009, 28, 587–597.

10 M. Crespo, M. Font-Bardia and X. Solans, Organometallics, 2004, 23, 1708–1713.

11 M. Font-Bardia, C. Gallego, M. Martínez and X. Solans, Organometallics, 2002, 21, 3305–3307.

12 C. Gallego, M. Martínez and V. S. Safont, Organometallics, 2007, 26, 527–537.

13 R. Cortés, M. Crespo, L. Davin, R. Martín, J. Quirante, D. Ruiz, R. Messeguer, C. Calvis, L. Baldomà, J. Badia, M. Font-Bardía, T. Calvet and M. Cascante, Eur. J. Med. Chem., 2012, 54, 557–566.

14 A. Escolà, M. Crespo, J. Quirante, R. Cortés, A. Jayaraman, J. Badía, L. Baldomà, T. Calvet, M. Font-Bardía and M. Cascante, Organometallics, 2014, 33, 1740–1750.

15 I. Omae in Cyclometallation reactions: Five membered ring products as universal reagents, Springer, 2014.

16 I. Omae, Coord. Chem. Rev., 2014, 280, 84–95.

17 M. Albrecht, Chem. Rev., 2009, 110, 576–623.

18 T. Calvet, M. Crespo, M. Font-Bardía, S. Jansat and M. Martínez, Organometallics, 2012, 31, 4367–4373.

19 M. Crespo, M. Martínez, S. M. Nabavizadeh and M. Rashidi, Coord. Chem. Rev., 2014, 279, 115–140.

20 J. Granell and M. Martínez, Dalton Trans., 2012, 41, 11243–11258.

21 R. N. Perutz and S. Sabo-Etienne, Angew. Chem., Int. Ed. 2007, 46, 2578–2592.

22 B. R. Steele and K. Vrieze, Transition Met. Chem., 1977, 2, 169–174.

23 C. M. Anderson, M. Crespo, M. C. Jennings, A. J. Lough, G. Ferguson and R. J. Puddephatt, Organometallics, 1991, 10, 2672–2679.

24 G. M. Sheldrick, Acta Crystallogr., Sect. A: Fundam. Crystallogr., 2008, 64, 112–122.

25 R. van Eldik, in Inorganic High Pressure Chemistry, ed. R. van Eldik, Elsevier, 1986, pp. 1–68.
26 J. Garcia-Amorós, M. Martínez, H. Finkelman and D. Velasco, J. Phys. Chem. B, 2010, 114, 1287–1293.
27 B. P. Macpherson, B. M. Alzoubi, P. V. Bernhardt, M. Martínez, P. Tregloan and R. van Eldik, Dalton Trans., 2005, 1459–1467.
28 I. Favier, M. Gómez, J. Granell, M. Martínez, M. Font-Bardía and X. Solans, Dalton Trans., 2005, 123–132.
29 R. A. Binstead, A. D. Zuberbuhler and B. Jung, SPECFIT32. [3.0.34], Spectrum Software Associates, Marlborough, MA, USA, 2005.
30 M. Maeder and P. King, ReactLab, Jplus Consulting Pty Ltd, East Fremantle, WA, Australia, 2009.
31 G. D. Roiban, E. Serrano, T. Soler, G. Aullón, I. Grosu, C. Cativiela, M. Martínez and E. P. Urriolabeitia, Inorg. Chem, 2011, 50, 8132–8143.
32 A. D. Becke, J. Chem. Phys., 1993, 98, 5648–5652.
33 C. Lee, W. Yang and R. G. Parr, Phys. Rev. B: Condens. Matter, 1988, 37, 785–789.
34 B. Miechlich, A. Sauvin, H. Stoll and H. Preuss, Chem. Phys. Lett., 1989, 157, 200–206.
35 J. Grimme, J. Anthony, S. Ehrlich and H. Krieg, J. Chem. Phys., 2010, 132, 154104.
36 M. J. Frisch, et al., GAUSSIAN 09 (Revision CD.01), Gaussian Inc., Wallingford CT, 2009.
37 P. C. Hariharan and J. A. Pople, Theor. Chim. Acta, 1973, 28, 213–222.
38 M. M. Francl, W. J. Petro, W. J. Hehre, J. S. Binkley, M. S. Gordon, D. J. DeFrees and J. A. Pople, J. Chem. Phys., 1982, 77, 3654–3665.
39 V. Rassolov, J. A. Pople, M. Ratner and T. L. Windus, J. Chem. Phys., 1998, 109, 1223–1229.
40 P. J. Hay and W. R. Wadt, J. Chem. Phys., 1985, 82, 299–310.
41 P. J. Hay and W. R. Wadt, J. Chem. Phys., 1985, 82, 270–283.
42 D. J. Tannor, B. Marten, R. Murphy, R. A. Friesner, D. Sitkoff, A. Nicholls, B. Honig, M. Ringnalda and W. A. Goddard, J. Am. Chem. Soc., 1994, 116, 11875–11882.
43 B. Marten, K. Kim, C. Cortis, R. A. Friesner, R. B. Murphy, M. N. Ringnalda, D. Sitkoff and B. Honig, J. Phys. Chem., 1996, 100, 11775–11788.
44 A. V. Marenich, C. J. Cramer and D. G. Truhlar, J. Phys. Chem. B, 2009, 113, 6378–6396.
45 K. A. Peterson, D. Figgen, E. Goll, H. Stoll and M. Dolg, J. Chem. Phys., 2003, 119, 11113–11123.
46 D. Figgen, K. A. Peterson, M. Dolg and H. Stoll, J. Chem. Phys., 2009, 130, 164108–164112.
47 A. D. McLean and G. S. Chandler, J. Chem. Phys., 1980, 72, 5639–5648.
48 R. Krishnan, J. S. Binkley, R. Seeger and J. A. Pople, J. Chem. Phys., 1980, 72, 650–654.
49 S. Hoops, S. Sahle, R. Gauges, C. Lee, J. Pahle, N. Simus, M. Singhal, L. Xu, P. Mendes and U. Kummer, Bioinformatics, 2006, 22, 3067–3074.
.

## Legends to figures

**Figure 1** Molecular structures of compounds (a) 7-II-Br,F, (b) II-Br,F (E form), and (c) II'-Br,F (Z form); hydrogen atoms have been omitted for clarity.

**Figure 2.** a) Eyring plot (60–90 °C) for the dependence of the rate constants of the steps monitored by UV-Vis spectroscopy on the 5-IV-Br,F → 7-II-Br,F reaction. (b) Pressure dependence ln k versus P for the same processes.

**Figure 3** Qualitative product concentration evolution over time for II'-X,H (X = Br, Cl) on the arbitrary time scale.

535 **SCHEME 1**

536

537

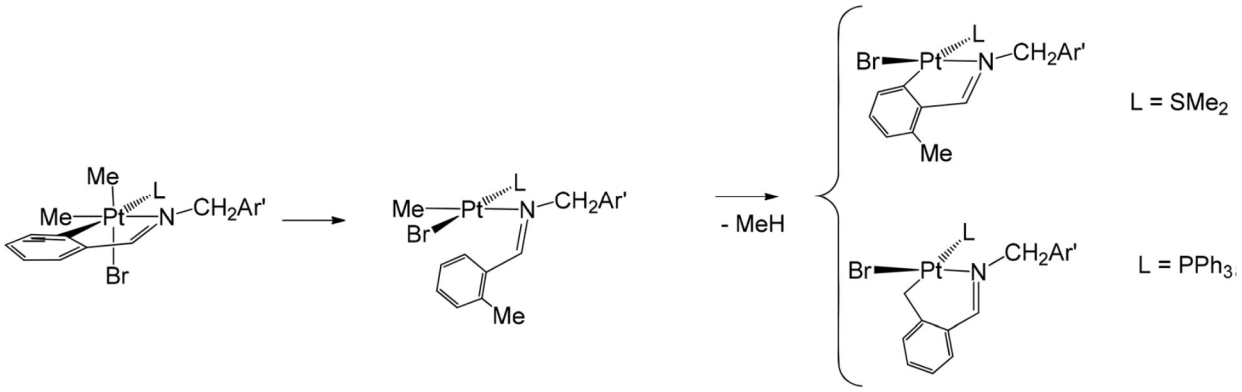


538

539

**SCHEME 2**

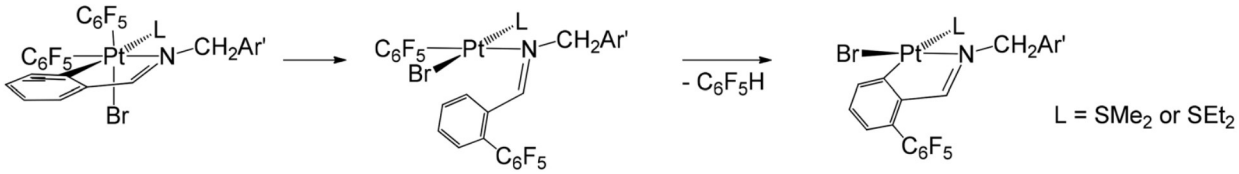
C6F5
L
C6F5
Pt
N
CH2Ar'
Br
C6F5
Pt
L
N
CH2Ar'
Br
C6F5
- C6F5H
Br
Pt
L
N
CH2Ar'
C6F5
L = SMe2 or SEt2

**SCHEME 3**

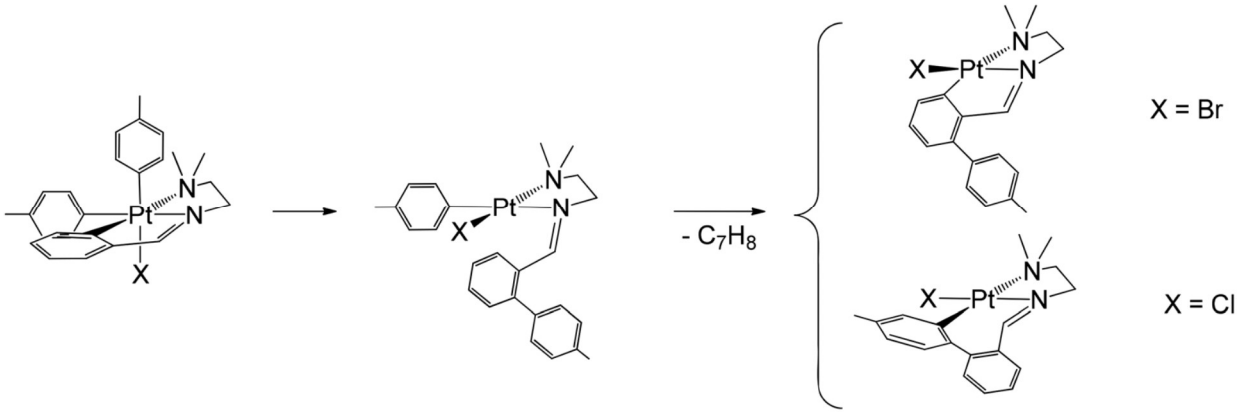

552 **SCHEME4**

553

554

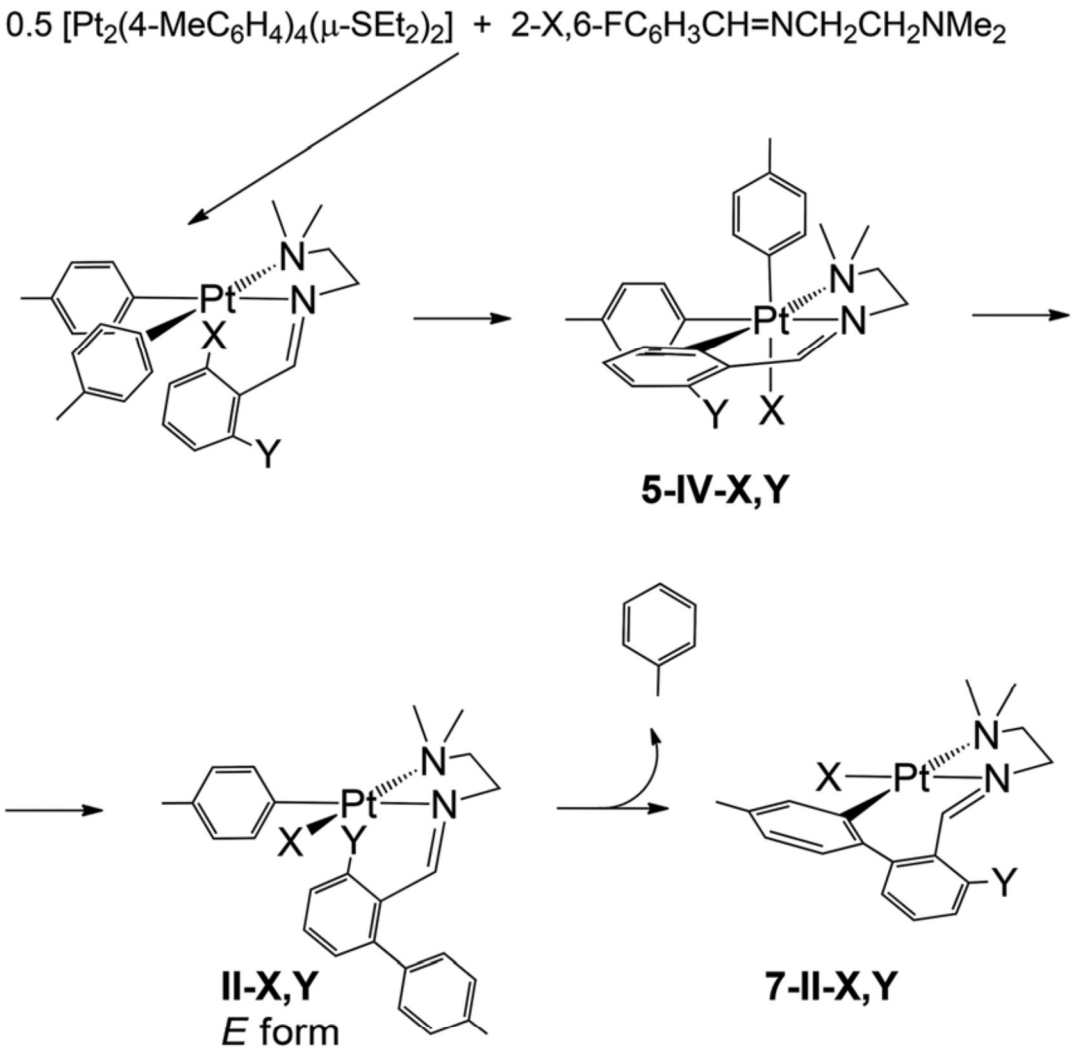


*Nomenclature* **(7, 5)-(II, IV)-X,Y** *for the complexes indicates*:

Number of members of the metallacycle for cyclometallated complexes (7, 5)

Oxidation state of the Platinum centre (II, IV)

Halide ligand attached to the Platinum centre (X)

555 Substituent in the non-metallated *ortho* position of the ArCH=$NCH_2CH_2NMe_2$ ligand (Y)

556

**FIGURE 1.**

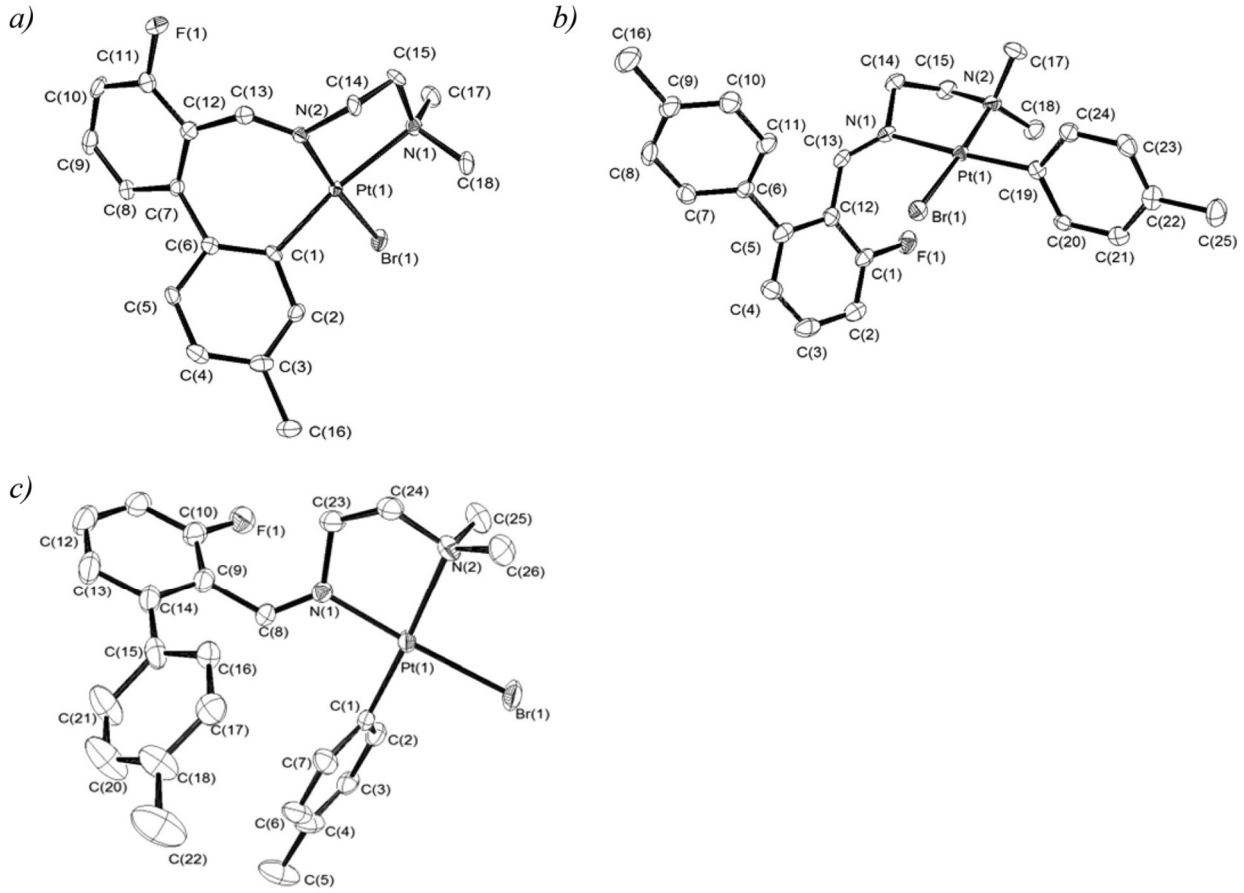
a)
F(1)
C(11)
C(15)
C(10)
C(12)
C(13)
C(14)
C(17)
N(2)
N(1)
C(9)
Pt(1)
C(18)
C(8)
C(7)
C(6)
C(1)
Br(1)
C(5)
C(2)
C(4)
C(3)
C(16)
b)
C(16)
C(14)
C(15)
C(17)
C(9)
C(10)
N(2)
C(18)
C(24)
C(11)
N(1)
C(13)
C(23)
C(8)
Pt(1)
C(19)
C(6)
C(12)
Br(1)
C(7)
C(22)
C(5)
F(1)
C(20)
C(25)
C(1)
C(21)
C(4)
C(2)
C(3)
c)
C(23)
C(24)
C(10)
F(1)
C(25)
C(12)
N(2)
C(26)
C(9)
C(13)
C(14)
N(1)
C(8)
C(15)
C(16)
Pt(1)
C(1)
Br(1)
C(21)
C(17)
C(2)
C(7)
C(18)
C(3)
C(20)
C(6)
C(4)
C(22)
C(5)

**SCHEME 5**

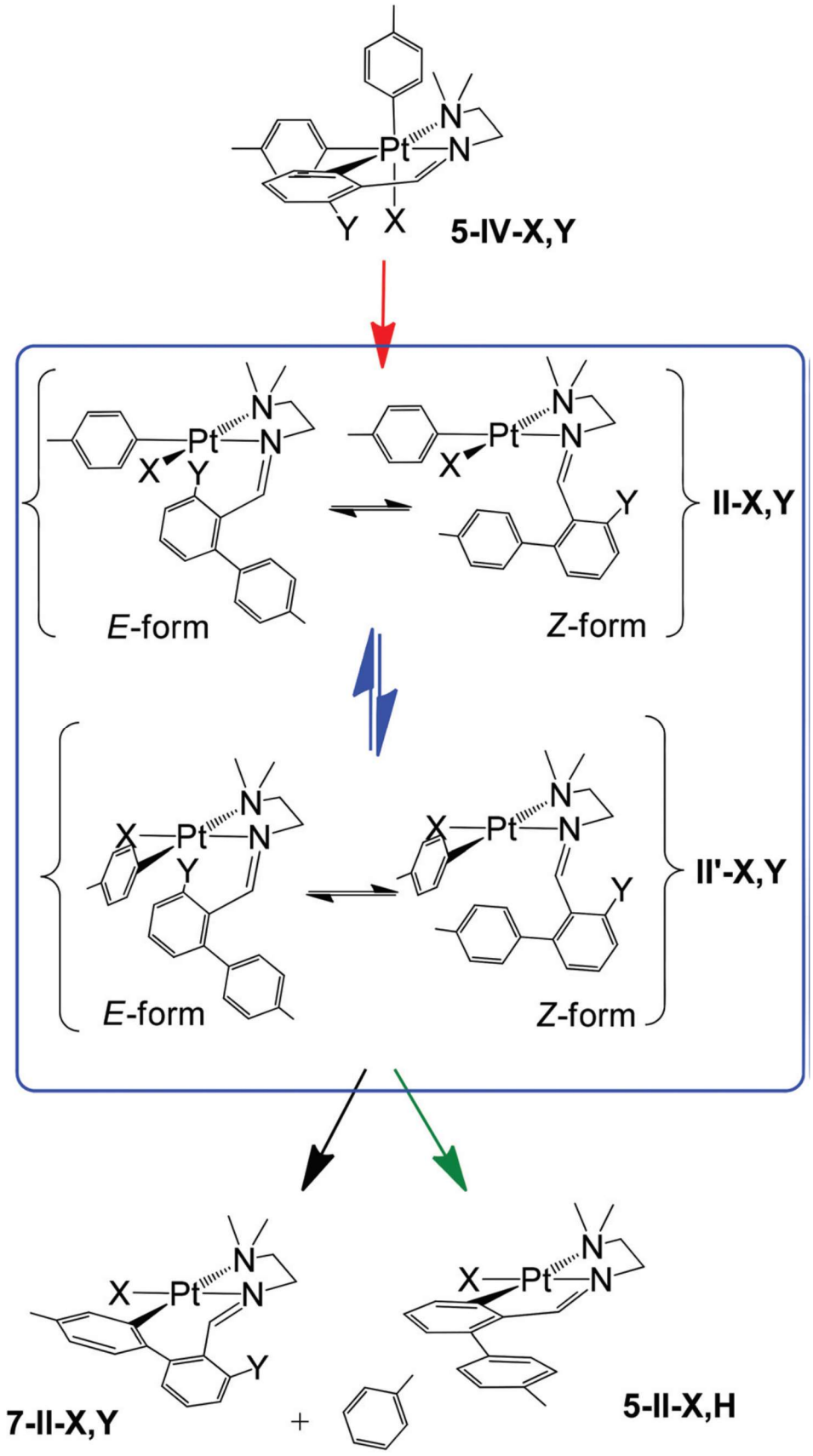

**FIGURE 2.**

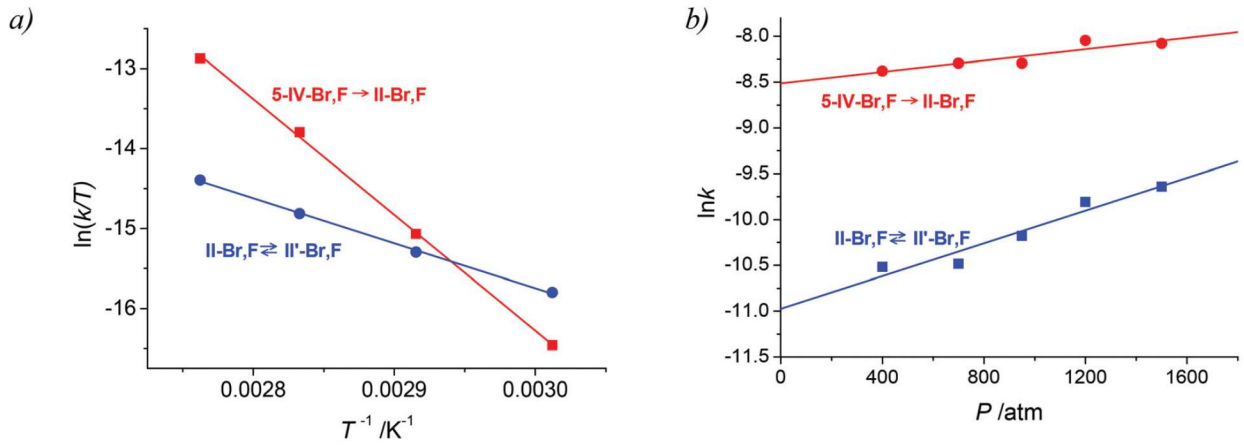
a)
ln(k/T)
-13
-14
-15
-16
0.0028
0.0029
0.0030
T -1 /K-1
5-IV-Br,F → II-Br,F
II-Br,F⇌ II'-Br,F
b)
lnk
-8.0
-8.5
-9.0
-9.5
-10.0
-10.5
-11.0
-11.5
0
400
800
1200
1600
P /atm
5-IV-Br,F → II-Br,F
II-Br,F⇌ II'-Br,F

572 **SCHEME 6**

573

574

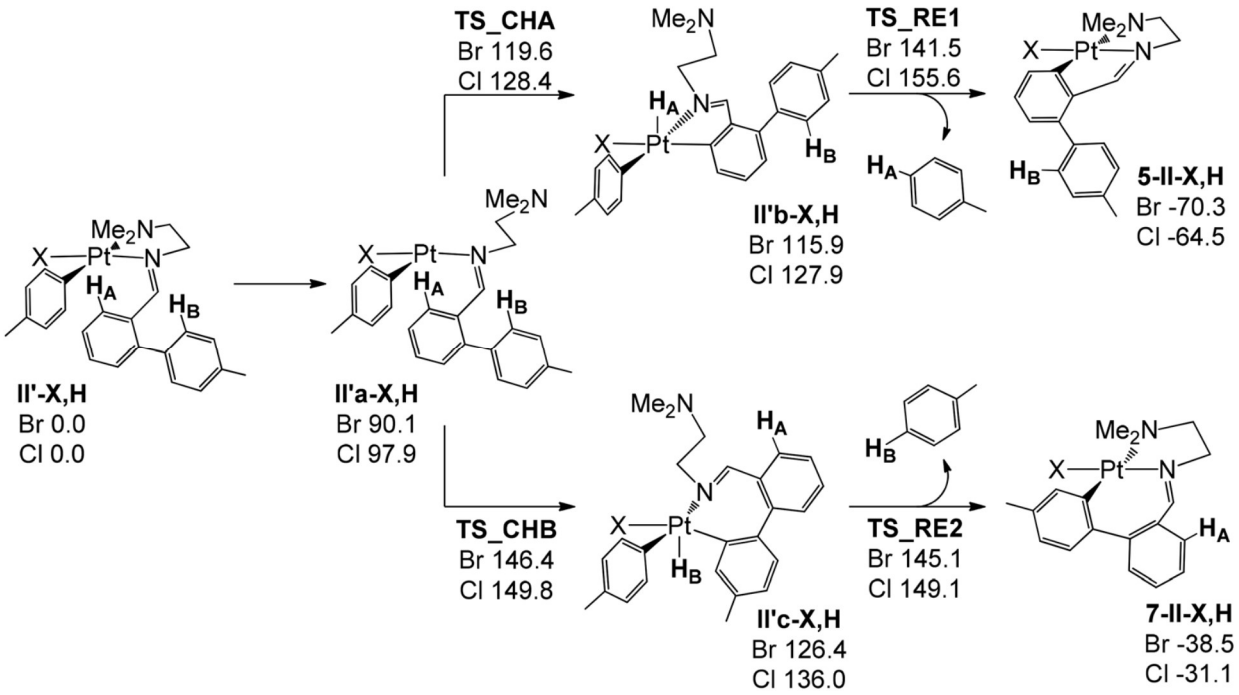


575

576

577 **FIGURE 3.**

578

579

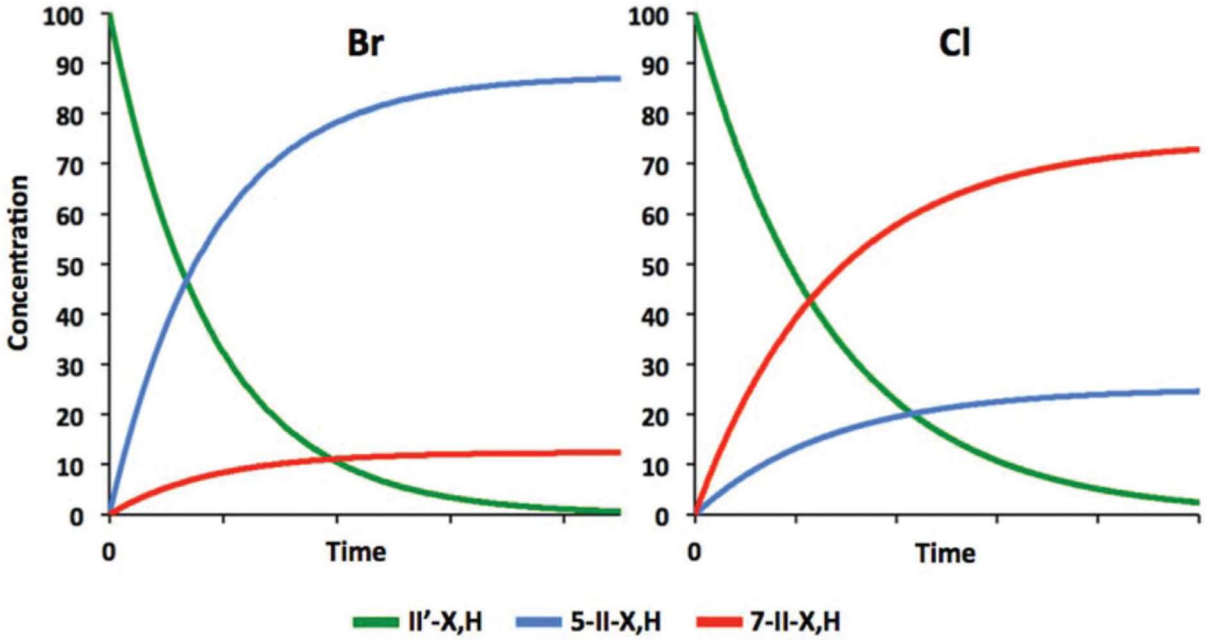


580

581

**CHART 1**

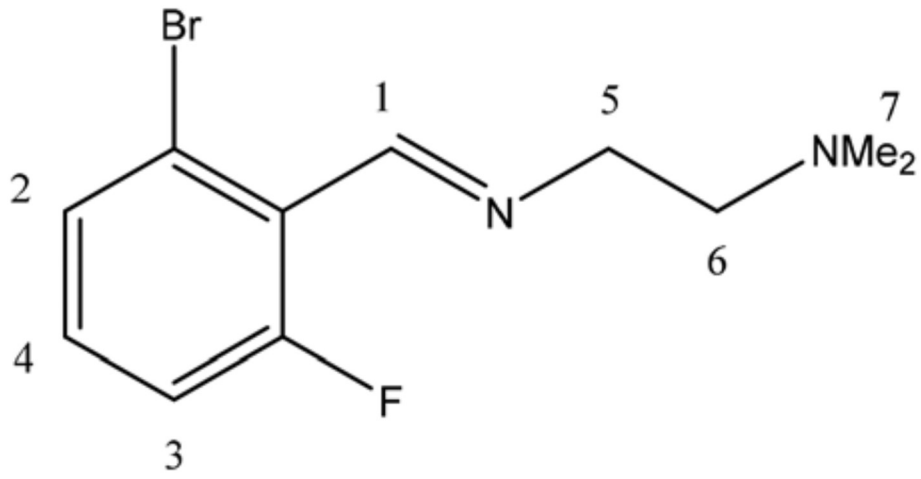

**CHART 2**

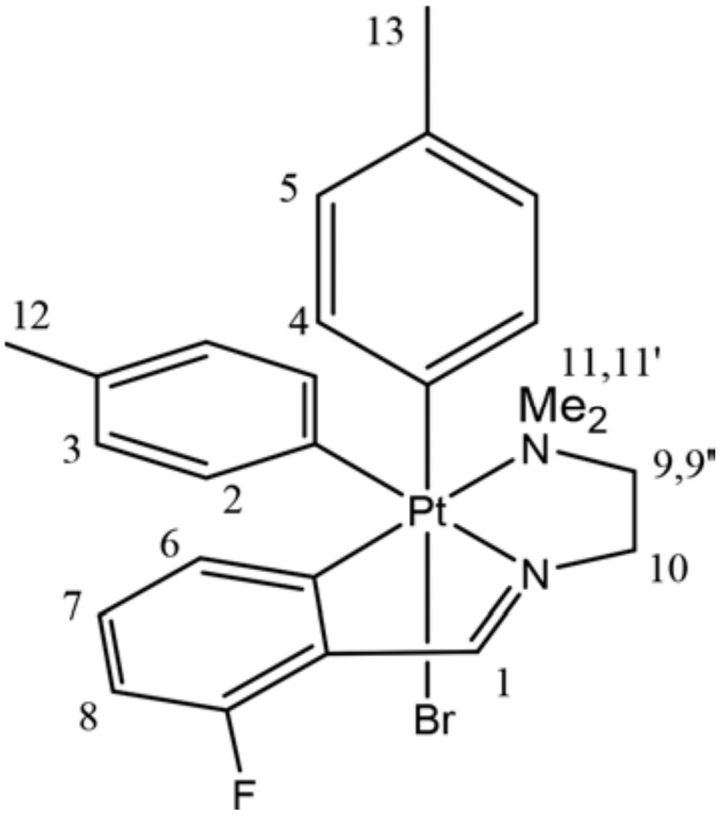

**CHART 3**

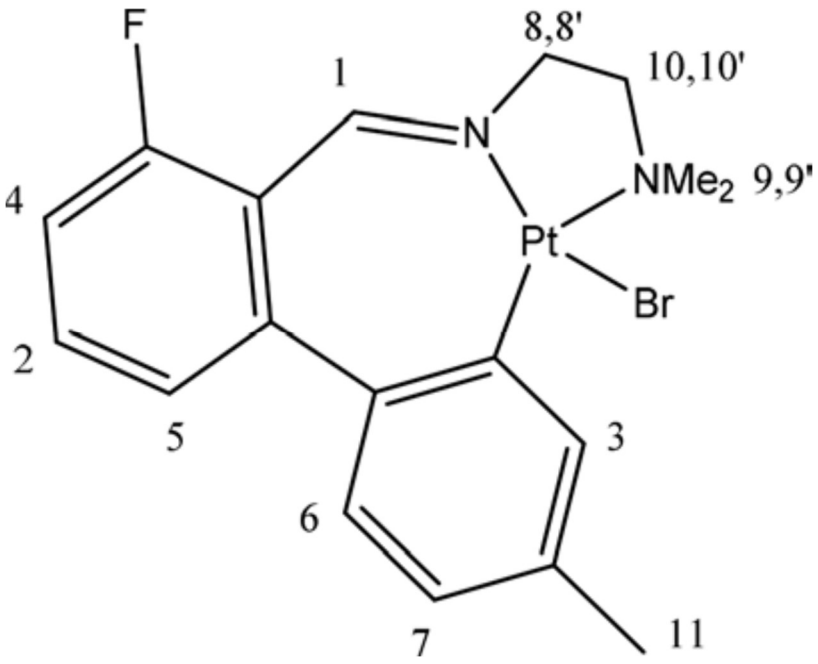

**CHART 4**

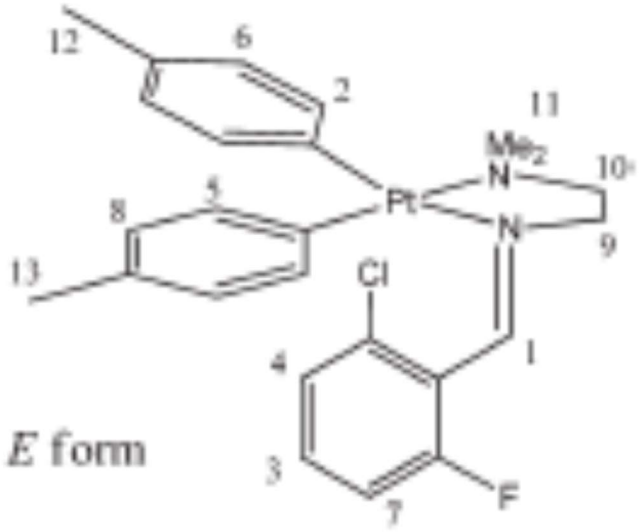


*E* form

**CHART 5**

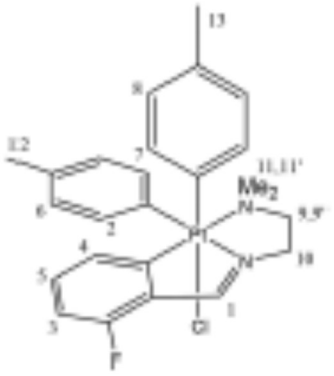

620 **CHART 6**

621

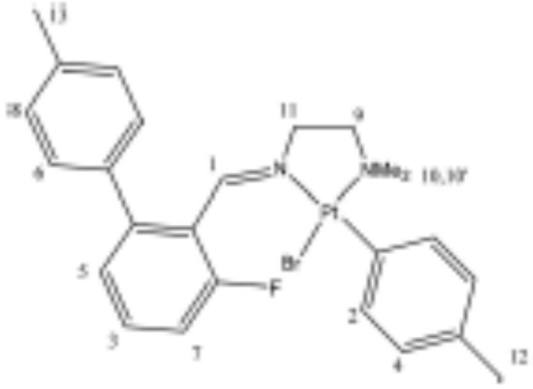


622

623

**Table 1.** Selected bond lengths (Å) and angles (°) for the structures determined for compounds 7-II-Br,F, II-Br,F (E form), and II'-Br,F (Z form)

| 7-II-Br,F | | II-Br,F (*E* form) | | II'-Br,F (*Z* form) | |
|---|---|---|---|---|---|
| Pt(1)–C(1) | 1.989(5) | Pt(1)–C(19) | 2.002(7) | Pt(1)–C(1) | 2.001(6) |
| Pt(1)–N(2) | 2.001(5) | Pt(1)–N(2) | 2.099(6) | Pt(1)–N(1) | 2.025(5) |
| Pt(1)–N(1) | 2.209(5) | Pt(1)–N(1) | 2.103(6) | Pt(1)–N(2) | 2.189(5) |
| Pt(1)–Br(1) | 2.4352(6) | Pt(1)–Br(1) | 2.4338(8) | Pt(1)–Br(1) | 2.4265(7) |
| N(1)–C(15) | 1.494(7) | N(1)–C(13) | 1.271(9) | N(1)–C(8) | 1.271(7) |
| N(2)–C(13) | 1.278(7) | N(1)–C(14) | 1.467(10) | N(1)–C(23) | 1.484(8) |
| N(2)–C(14) | 1.478(7) | N(2)–C(15) | 1.506(10) | N(2)–C(24) | 1.487(8) |
| C(1)–C(6) | 1.413(7) | C(14)–C(15) | 1.510(11) | C(23)–C(24) | 1.506(9) |
| C(6)–C(7) | 1.488(7) | C(19)–Pt(1)–N(2) | 93.7(3) | C(1)–Pt(1)–N(1) | 93.9(2) |
| C(7)–C(12) | 1.408(8) | N(2)–Pt(1)–N(1) | 82.0(2) | N(1)–Pt(1)–N(2) | 82.9(2) |
| C(12)–C(13) | 1.474(8) | C(19)–Pt(1)–Br(1) | 88.0(2) | C(1)–Pt(1)–Br(1) | 89.51(15) |
| C(14)–C(15) | 1.511(8) | N(1)–Pt(1)–Br(1) | 96.32(17) | N(2)–Pt(1)–Br(1) | 93.68(14) |
| C(1)–Pt(1)–N(2) | 91.8(2) | | | | |
| N(2)–Pt(1)–N(1) | 83.00(18) | | | | |
| C(1)–Pt(1)–Br(1) | 93.76(15) | | | | |
| N(1)–Pt(1)–Br(1) | 92.20(12) | | | | |

**Table 2** Kinetic and thermal activation parameters for the two reaction steps observed for the reaction of different 5-IV-X,Y leading to 7-II-X,Y according to Scheme 5 in xylene solution. * indicates a mixture of II-X,Y and II'-X,Y isomers7

| Reaction | Assignment | $10^5 \times {}^{340}k/s^{-1}$ | $\Delta H^{\ddagger}$/kJ mol$^{-1}$ | $\Delta S^{\ddagger}$/J K$^{-1}$ mol$^{-1}$ | $\Delta V^{\ddagger}$/cm$^3$ mol$^{-1}$ |
|---|---|---|---|---|---|
| 5-IV-Cl,H → 7-II-Cl,H[4] | 5-IV-Cl,H → II-Cl,H* | 9.1 | 122 ± 5 | 33 ± 13 | Not determined |
| | II-Cl,H* → 7-II-Cl,H | 0.29 | 141 ± 15 | 60 ± 44 | Not determined |
| 5-IV-Cl,Cl → 7-II-Cl,Cl[4] | 5-IV-Cl,Cl → II-Cl,Cl* | 3.4 | 118 ± 5 | 13 ± 13 | Not determined |
| | II-Cl,Cl* → 7-II-Cl,Cl | 29 | 102 ± 5 | −16 ± 15 | Not determined |
| 5-IV-Br,H → 5-II-Br,H[4] | 5-IV-Br,H → II-Br,H | 240 | 97 ± 4 | −13 ± 11 | Not determined |
| | II-Br,H ⇄ II'-Br,H | 150 | 42 ± 5 | −179 ± 15 | Not determined |
| | II-Br,H* → 5-II-Br,H | 30 | 86 ± 7 | −63 ± 20 | Not determined |
| 5-IV-Br,F → 7-II-Br,F this work | 5-IV-Br,F → II-Br,F | 7.1 | 121 ± 2 | 28 ± 7 | −9 ± 2 at 333 K |
| | II-Br,F ⇄ II'-Br,F | 7.1 | 54 ± 4 | −169 ± 12 | −24 ± 4 at 328 K |
| 5-IV-Cl,F → 7-II-Cl,F this work | 5-IV-Cl,F → II-Cl,F | 55 000 | 69 ± 15 | −50 ± 45 | Not determined |
| | II-Cl,F ⇄ II'-Cl,F | 1.8 | 63 ± 5 | −154 ± 13 | Not determined |
| | II'-Cl,F → 7-II-Cl,F | 2200 | 106 ± 15 | 32 ± 40 | Not determined |

641 **Table 3** Computed relative free energies (kJ mol−1 at 139 °C) for the E and Z forms of the II-X,H and
642 II'-X,H compounds indicated in Scheme 5
643

| | X = Br | | X = Cl | |
|---|---|---|---|---|
| | *E* form | *Z* form | *E* form | *Z* form |
| **II-X,H** | 17.0 | 15.8 | 33.0 | 32.3 |
| **TS_Isom** | 138.4 | Not calculated | 140.1 | Not calculated |
| **II'-X,H** | 0 | 7.5 | 0 | 12.1 |

644
645
646

**Table 4** Crystallographic and refinement data for compounds 7-II-Br,F, II-Br,F (E form), and II'-Br,F (Z form)

| | 7-II-Br,F | II-Br,F (*E* form) | II-Br,F (*Z* form) |
|---|---|---|---|
| Formula | $C_{18}H_{20}BrFN_2Pt$ | $C_{25}H_{28}BrFN_2Pt$ | $C_{25}H_{28}BrFN_2Pt$ |
| Fw | 558.36 | 735.42 | 735.42 |
| Temp., K | 100 (K) | 100(2) | 100(2) |
| Wavelength | 0.71073 | 0.71073 | 0.71073 |
| Crystal system | Monoclinic | Monoclinic | Monoclinic |
| Space group | *P*21/*c* | *C*2/*c* | *C*2/*c* |
| *a* | 10.1118(10) | 27.163(2) | 26.7638(14) |
| *b* | 28.201(3) | 15.4717(11) | 13.0691(7) |
| *c* | 15.4709(13) | 13.4316(11) | 15.8211(8) |
| *β*, ° | 127.177(5) | 109.882(3) | 117.052(2) |
| *V*; *Z* | 3515.1(6); 8 | 5308.4(7); 8 | 4928.4(5); 8 |
| *d* (calcd) | 2.11 | 1.84 | 1.753 |
| Abs. Coeff., mm | 10.266 | 7.018 | 7.336 |
| *F* (000) | 2112 | 2848 | 2512 |
| Rflns coll./unique | 52 682/8740 [*R*(int) = 0.0635] | 75 357/6599 [*R*(int) = 0.0871] | 70 645/8610 [*R*(int) = 0.0702] |
| Data/restraint/parameter | 8740/1/421 | 6599/0/302 | 8610/1/275 |
| GOF on *F* | 1.113 | 1.097 | 1.045 |
| Final *R* [*I* > 2*σ*(*I*)] | $R_1$ = 0.0390 | $R_1$ = 0.0569 | $R_1$ = 0.0562 |
| | w$R_2$ = 0.0593 | w$R_2$ = 0.1050 | w$R_2$ = 0.0969 |
| *R* (all data) | $R_1$ = 0.0557 | $R_1$ = 0.0738 | $R_1$ = 0.0883 |
| | w$R_2$ = 0.0642 | w$R_2$ = 0.1120 | w$R_2$ = 0.1094 |
| Peak and hole | 1.058 and −1.033 | 5.981 and −1.677 | 4.455 and −2.517 |
| CDCC number | 1051232 | 1051233 | 1051234 |